Journal of the Meteorological Society of Japan, Vol.79, No.2, pp.687–694, 2001

NOTES AND CORRESPONDENCE

Estimation of Surface Heat Flux Based on Rawinsonde Observation in the Southwestern Part of the Sea of Okhotsk under Ice-covered Condition

By Katsushi Iwamoto

Graduate School of Environmental Earth Science, Hokkaido University, Sapporo, Japan

Kei Domon

Research Institute of Civilization, Tokai University, Hiratsuka, Japan

Meiji Honda

Institute for Global Change Research, Frontier Research System for Global Change, Tokyo, Japan

Yoshihiro Tachibana

IARC, Frontier Research System for Global Change, Tokyo, Japan,
Research Institute of Civilization, Tokai University, Hiratsuka, Japan

and

Kensuke Takeuchi

Institute of Low Temperature Science, Hokkaido University, Sapporo, Japan

(Manuscript received 21 July 2000, in revised form 21 November 2000)

Abstract

Rawinsonde observation was performed in late January through early February in 1998 around the southwestern part of the Sea of Okhotsk to estimate the turbulent fluxes of sensible and latent heat over the ice-covered ocean during the winter monsoon. Upstream cold and stable air mass originated from the Eurasian continent was significantly modified through heat and moisture supply from warm sea surface with offshore cold-air outbreaks, which consequently formed mixed layer characterized by neutral stability over downstream areas. Associated with reduction of the top of the mixed layer height through the observational period, estimated heat fluxes also decreased gradually from 210 W m^{-2} to 30 W m^{-2}. These decrease tendencies of the mixed layer height and estimated heat fluxes may reflect the increase of the insulating effect of the sea-ice cover on heat and moisture exchanges between the atmosphere and ocean.

Corresponding author: Katsushi Iwamoto, Institute of Low Temperature Science, Hokkaido University, Kita19, Nishi8, Sapporo, 060–0819, Japan.
E-mail: katsu@lowtem.hokudai.ac.jp

1. Introduction

The Sea of Okhotsk, which is located between about 45–60°N, is extensively covered with sea ice during winter. The winter monsoon from the

Eurasian continent associated with the combination of the Aleutian low and Siberian high acts to increase the sea-ice cover through a cold northerly advection and an offshore wind stress. It is well known that the interannual variability of the atmospheric circulation over the Far East causes large fluctuations in the Okhotsk sea-ice cover (e.g., Cavalieri and Parkinson 1987; Parkinson 1990; Fang and Wallace 1994). Conversely, the sea-ice cover may be capable of influencing the atmospheric field. Sea ice significantly reduces a heat exchange between the atmosphere and ocean, and it consequently cools the air mass above. Significant atmosphere-ocean energy exchanges are expected over the open ocean off the ice-edge when cold air outbreaks occur. Several previous studies suggested that anomalous Okhotsk sea-ice cover may influence air temperatures and/or snowfall processes over and around Hokkaido (e.g., Nagata and Ikawa 1988; Sasaki and Deguti, 1988; Honda et al. 1994; Okubo and Mannoji 1994), although these studies are limited to local influence of the sea ice on the atmosphere. Recently, Honda et al. (1996; 1999), using an atmospheric general circulation model, showed that the Okhotsk sea-ice cover anomalies bring about significant large-scale atmospheric responses not only around the Sea of Okhotsk but also downstream towards North America. This remote response is caused by anomalous turbulent heat flux off the ice-edge over and around the Sea of Okhotsk associated with sea-ice extent anomalies. They also showed that similar atmospheric patterns are obtained in composite anomalies of observational atmospheric fields associated with observed sea-ice cover anomalies. This result suggests that the seasonal and interannual variability of sea-ice distribution influences large-scale atmospheric fields through the variability of the distribution of the heat flux at the lower boundary. Several observational studies have estimated the turbulent heat fluxes of sensible and latent heat over the open ocean off the ice-edge in offshore wind conditions in other marginal ice zone (MIZ), for example, in the Bering Sea (e.g., Hein and Brown 1988) and the Greenland Sea (e.g., Kellner et al. 1987; Brümmer 1996). However, few heat flux measurements have existed in wintertime ice-covered conditions in the Sea of Okhotsk which is also a typical MIZ. Furthermore, atmospheric modifications with these fluxes over the Sea of Okhotsk have not been investigated at all during winter.

The purpose of this study is to estimate the turbulent heat fluxes in the Sea of Okhotsk covered with sea ice, and to investigate processes of the boundary-layer modification over there, when the cold air outbreaks from the Eurasian continent occur. For this purpose, the first systematic atmospheric observation using rawinsondes in the southwestern part of the Sea of Okhotsk was performed from late January to early February in 1998, when sea ice reached and covered the Okhotsk coast of Hokkaido, Japan. In this short contribution, we focus on the heat flux estimation over the Sea of Okhotsk using the obtained rawinsonde data as a preliminary result.

2. Observation

Cold-air outbreaks are intermittent southward or southeastward cold advections from eastern Siberia, the coldest region in the Northern Hemisphere, caused by a zonal pressure gradient after the passage of the extra-tropical cyclones to eastward of Japan. In order to investigate the air mass modification along the directions of the cold-air advection, we developed three rawinsonde stations (two land-based and one shipboard) along mean wind directions for the climatic mean winter monsoon around the southwestern part of the Sea of Okhotsk (Fig. 1) in the winter of 1998. One land-based station is Yuzhno-Sakhalinsk (hereafter YS; 46.9°N and 142.7°E), a Russian meteorological observatory, which is located upstream of the winter monsoon in the observational area. The northwestern part of the Sea of Okhotsk, including the northernmost part of the Sea of Japan, is almost perfectly covered with sea ice during winter. An air mass observed at YS with a northerly wind component is, therefore, expected to retain its characteristics which originated from eastern Siberia, because the ice cover insulates heat fluxes from the ocean. Another land-based station is temporally developed at Shari, the Okhotsk coast of Hokkaido (hereafter SH; 43.9°N and 144.6°E). SH is at the lowest latitude of the Sea of Okhotsk (Fig. 1), and is located downstream of the winter monsoon passing over YS. In normal years, the southern edge of the sea-ice cover reaches the Okhotsk coast of Hokkaido around the end of January, and the sea ice extensively covers almost all the coastal area by mid-February. So, we can observe the reduction of heat and moisture fluxes from the sea surface due to the increase of sea-ice coverage by comparing the vertical profile of an air mass observed over SH with that of YS through this period. For this reason,

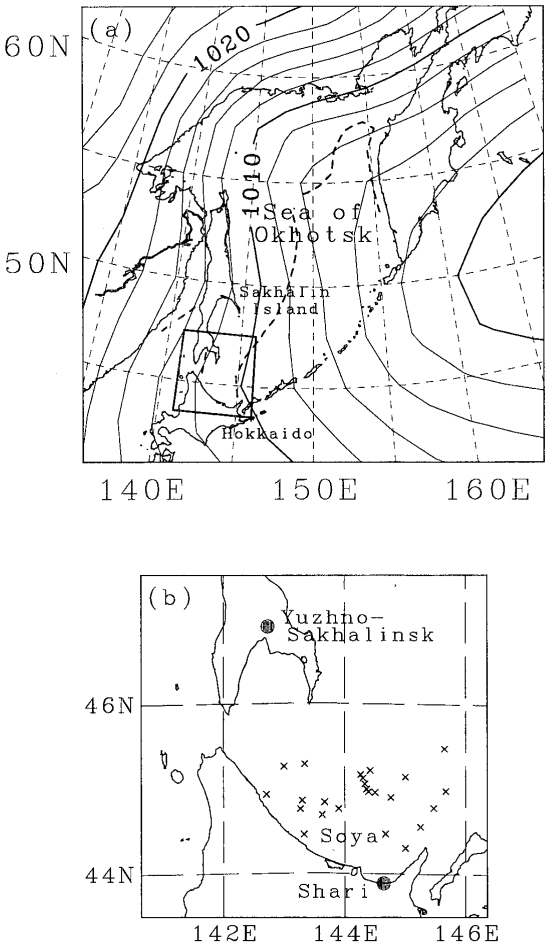

Fig. 1. Location map of (a) the Sea of Okhotsk and of (b) the observational area. Solid lines in (a) indicate mean sea level pressure (hPa) in January for 1967–1997. Mean sea-ice edge for the end of January (1979–1998), which is indicated by 40% ice concentration, is shown by dashed lines. Solid circles and crosses in (b) represent land-based stations and ship-based station on the ice breaker *Soya* (SO), respectively.

we performed rawinsonde soundings from 26 January to 11 February 1998 at the two land-based stations. Soundings were made four times a day (00 UTC, 06 UTC, 12 UTC, and 18 UTC) through the observational period. Since twice observations daily (00 UTC and 12 UTC) are operationally performed at YS, we requested the Russian Weather Service to perform two soundings daily additional at YS (06 UTC and 18 UTC). Moreover, four more observations a day (03 UTC, 09 UTC, 15 UTC, and 21 UTC) were added at SH when the cold-air outbreaks occurred (from 18 UTC 3 to 00 UTC 7 February, from 18 UTC 8 to 06 UTC 9 February, and from 12 UTC 10 to 06 UTC 11 February), to obtain higher time resolution for vertical profiles of the air mass, during the outbreaks.

The ice breaker *Soya*, which belongs to the Japan Maritime Safety Agency (currently, Japan Coast Guard), patrols the Sea of Okhotsk off Hokkaido during the arrival period of sea ice every year. We developed the shipboard station on the *Soya* (hereafter SO) during her cruise, and performed four or eight times rawinsonde observations a day from 4 to 11 February. The area of her cruise was mostly within the southwestern part of the Sea of Okhotsk, which almost corresponds to the midstream area of the climatic-mean cold northerly between YS and SH (Fig. 1). Therefore, the obtained data at SO may intrinsically reflect the actually modified air mass over the ice-covered ocean between YS and SH.

3. Synoptic situation

Figure 2 shows the time series of vertical profiles of the air temperature and horizontal wind vector which were obtained by the rawinsonde observation at YS and SH (Figs. 2a and 2b, respectively), and the temperature difference between YS and SH (Fig. 2c). On the basis of weather charts (not shown), extra-tropical cyclones periodically passed near Hokkaido during our observation. Cold-air outbreaks after the passage of the cyclones, which are identified as northerly winds and colder air temperatures in the lower troposphere, occurred four times: from 26 to 29 January, from 31 January to 1 February, from 4 to 6 February, and from 10 February to the end of the observation (Figs. 2a and 2b, horizontal lines at the top of each panels). Nearly simultaneous variations of the temperature through the layer at YS and SH may reflect the behavior of these cyclones.

The wind direction observed at YS was almost northerly in the lower layer irrespective of the temperature variation (Fig. 2a), which suggests that the air mass originated from the eastern Siberia was dominant in the lower layer at YS. Furthermore, the surface inversions which is indicated as lower air temperature near surface than that above frequently developed at YS (Fig. 2a, or more clearly identified in Fig. 2c), which indicates that the lower-layer air mass is not substantially influenced by heat release from the ocean. On the other hand, the northerly and southerly wind component corresponded to the decrease and increase of the tem-

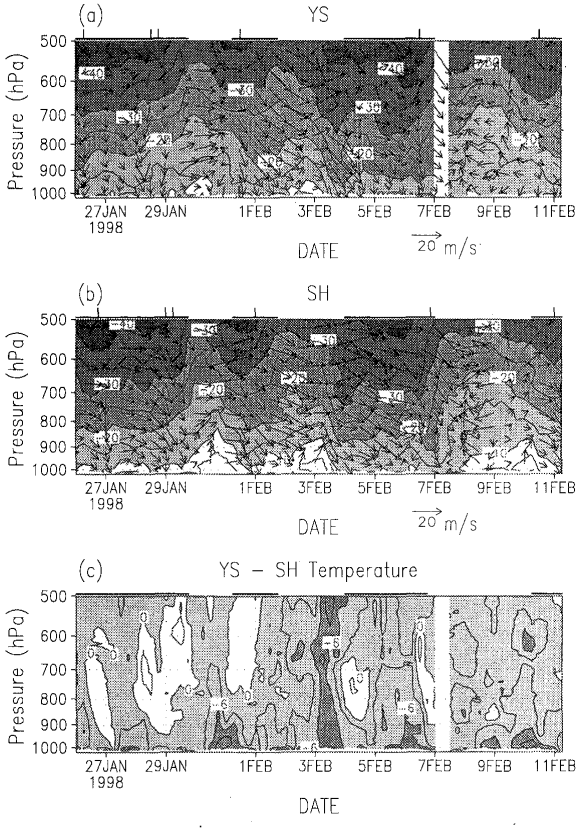

Fig. 2. Vertical-time cross sections of observed air temperature (℃; contours) and horizontal wind vector (arrows) at (a) Yuzhno-Sakhalinsk (YS) and (b) Shari (SH) and (c) temperature difference between YS and SH. Contour interval is 5 ℃ for (a) and (b), and 3 ℃ for (c). Horizontal lines at the top of each panel indicate the periods of cold-air outbreaks, and vertical lines at the top of the panels (a) and (b) indicate the six cases indicated in Fig. 4a.

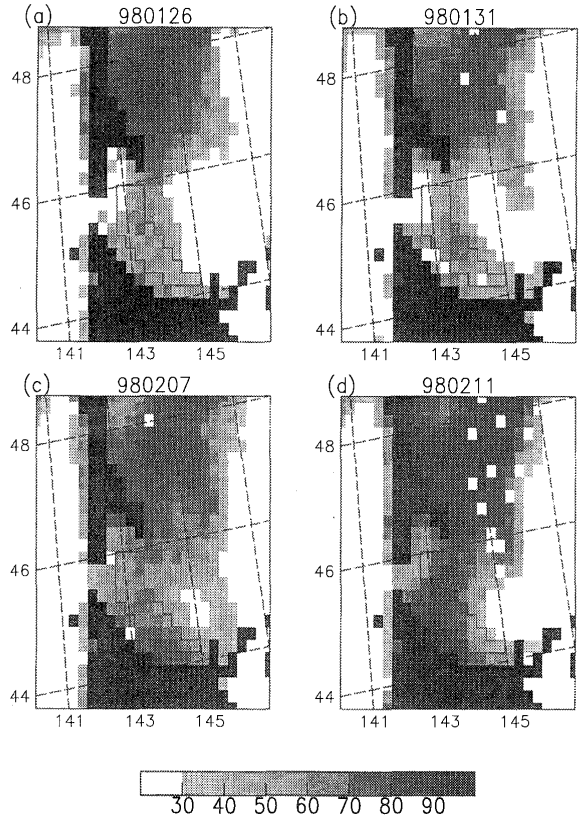

Fig. 3. Sea-ice concentration (%) around the southwestern part of the Sea of Okhotsk derived from Defense Meteorological Satellite Program's (DMSP) Special Sensor Microwave/Imagers (SSM/I): (a) 26 January, (b) 31 January, (c) 7 February, (d) 11 February.

perature in the lower layer at SH (Fig. 2b). Moreover, the lower-layer temperature at SH was systematically higher than that at YS throughout the observational period (Fig. 2c). Mean temperature differences between SH and YS during the whole period is 1.3 ℃ at 700 hPa level and 5.2 ℃ at 1000 hPa level, which indicates that the air mass stability of SH was generally weak compared with that of YS. These facts imply that the cold air mass originated from eastern Siberia at YS reached SH with modification from the ocean, at least in the four cold phases.

Figure 3 shows the distribution of sea-ice concentration on (a) 26 January, (b) 31 January, (c) 7 February, and (d) 11 February. The sea-ice data, DMSP–F13 Daily Sea Ice Concentrations 1998, was obtained from the EOSDIS NSIDC Distributed Active Archive Center (NSIDC DAAC), University of Colorado at Boulder (published by National Snow and Ice Data Center 1989). During our observation, the sea-ice coverage between Sakhalin and Hokkaido increased considerably by advection associated with the continual northerly wind near the surface (Fig. 2a). At the beginning, the mean sea-ice concentration in the area enclosed by thin lines in Fig. 3[1] was 45–50% and open water area extended to the east of Soya Strait (Figs. 3a and 3b). By the end of our observation, the area was mostly covered with sea ice, and the mean ice concentration increased up to 71% and exceeded 80% at maximum between Sakhalin and the Okhotsk coast of Hokkaido (Fig. 3d).

4. Heat flux estimation

4.1 Mixed layer development

Associated with cold-air outbreaks, cold and stable air mass originated from the eastern Siberia undergoes significant modification by heat and moisture supply from the warm sea surface. Heating from the bottom destabilizes the atmospheric boundary layer, and consequently forms mixed layer through convective processes. However, the sea ice reduces the development of the mixed layer by insulating the heat exchange between the sea surface and the atmosphere.

The mixed layer is easily identified as neutral stability in the vertical profile of equivalent potential temperature. We first chose the cases satisfying both conditions that the mixed layer was identified at SH and the wind was blowing from YS (or SO) to SH at the lower level. The latter was confirmed in a backward trajectory analysis from SH, using wind data at 925 hPa of the Europian Centre for Medium-Range Weather Forecasts (ECMWF) analyses. Since we used a $0.5° \times 0.5°$ grid data set to calculate each of the air-mass trajectories, we permitted the case that the trajectory passes within the ranges of 50 km from YS (or SO) and SH (Fig. 4). In this manner, we obtained nine cases. It is indicated in Fig. 4 that air mass advection takes about 9 or 12 hours from YS to SH, and about 3 hours from SO to SH. Then, considering the time lag for the advection between two stations in each case, we picked the pair of soundings at both sites and compared their vertical profiles of equivalent potential temperature. As our observation at YS and SO was performed every 3 or 6 hours, there does not necessarily exist the corresponding sounding at YS (or SO) with the estimated time lag, so we chose the closest one. Figure 5 shows thus-selected profiles of the equivalent potential temperature at YS (or SO) and SH. Clear modifications can be identified from YS (or SO) to SH (Fig. 5), i.e., stable stratification at YS (or SO), clear mixed layer at SH, and similar profiles of free atmosphere above the mixed layer at SH and YS (or SO). Hereafter, these nine cases are named as *case 1*, *2*, $\cdots$, and *case 9*, respectively.

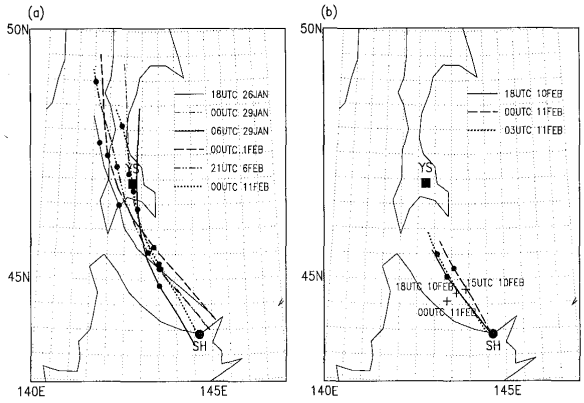

Fig. 4. Backward trajectories from SH based on wind data at 925 hPa of the European Centre for Medium-Range Weather Forecasts (ECMWF) $0.5° \times 0.5°$ grid analyses. The interval between two closed circles is 6 hours. Times that the air masses are located at SH are shown in both panels. (a): from SH to YS. (b): from SH to SO.

Based on the profiles in Fig. 5, the top of the mixed layer of SH in each case was decided based on the squared buoyancy frequency, and we adopted 1.5×10^{-4} (sec^{-2}) as its threshold. It is indicated as the horizontal thin line in each panel of Fig. 5, and in Table 1. The thickness of the mixed layer of SH has a decreasing tendency with time during the observation. This tendency seems to correspond to increase of the ice concentration by about 30% during the observation (Fig. 3 and Table 1).

4.2 Surface heat flux

The development of the mixed layer is influenced by various conditions, e.g., initial stability at the upstream station, sea-surface condition, existence of cloud, radiative effect, and so on. The mixed layer develops mainly by the heat and moisture supply from the sea surface between YS and SH.

The heat and moisture supply should reflect the moist static energy h of the air mass, which is defined as $h = c_pT + L_cq + gz$. When the air mass at YS moves to SH, the air-mass modification occurs in the layer between the lower boundary, p_{low}, and the top of the mixed layer at SH, p_{top}, and the total increment of the moist static energy, ΔH, is represented as follows:

$$\Delta H = -\int_{p_{low}}^{p_{top}} \frac{1}{g}\left(h_{SH} - h_{YS}\right) dp, \qquad (1)$$

where subscripts denote the stations. The total en-

1 Sea-ice area which does not exist in the real condition often appears on grids adjacent to the mid-latitude coast in this ice dataset, which may be related to substantial problems both of the field of view of the sensor and used algorithm. So we excluded the ice concentration values near the coast when we calculated the area-averaged values in this area.

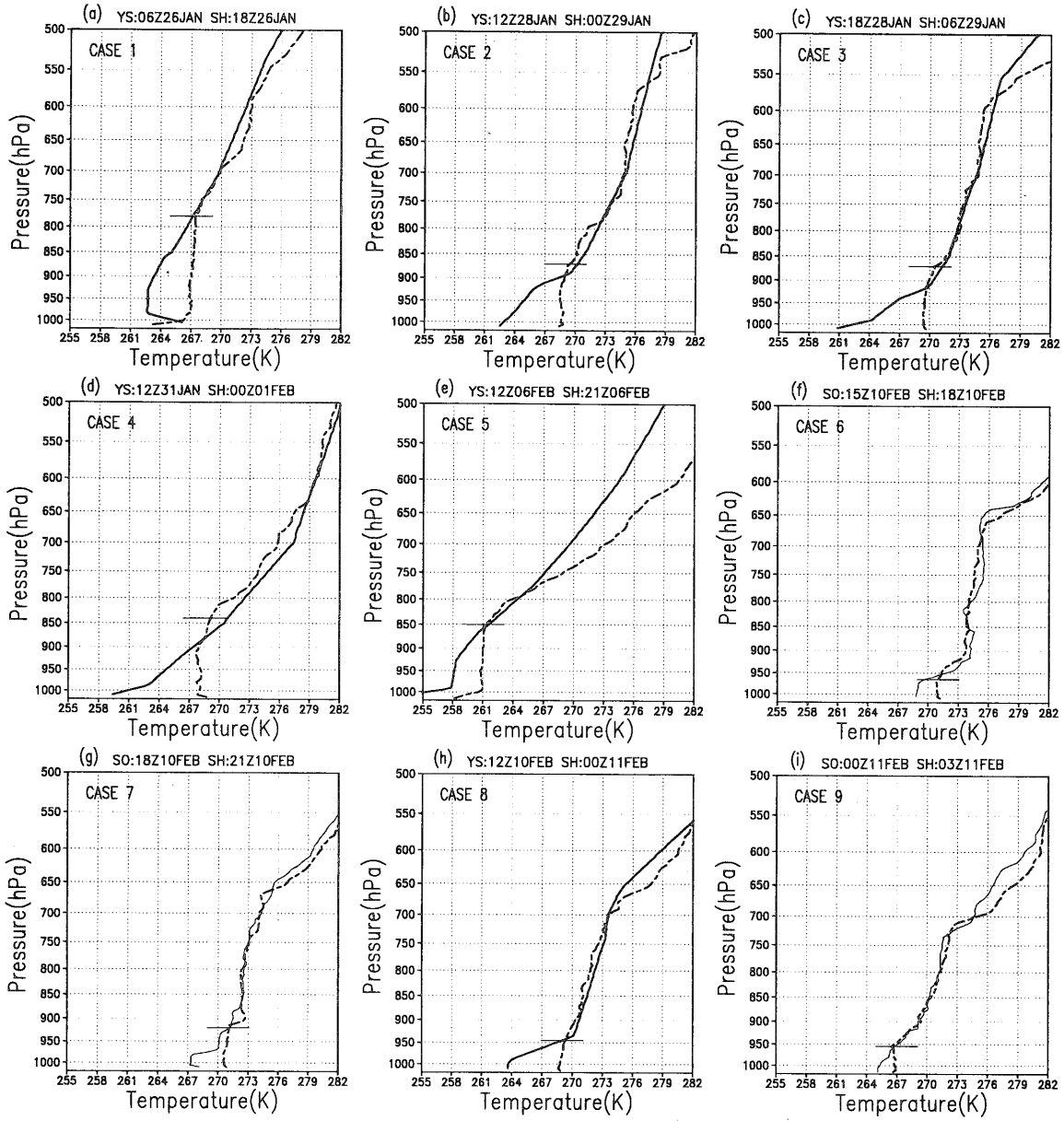

Fig. 5. Vertical profiles of equivalent potential temperature at YS (thick solid line), SO (thin solid line), and SH (dashed line). Horizontal thin lines denote the top of the mixed layer.

ergy increment is mainly due to the sensible and latent heat fluxes and the radiation effect. So, we extract the turbulent fluxes of the sensible and latent heat (F) by removing the effect of heating/cooling by the radiation process, that is,

$$F = \frac{\Delta H}{\Delta t} - F_{rad}, \tag{2}$$

where Δt is the time lag for the air mass advecting between the stations and F_{rad} is the net radiative flux in the mixed layer. To estimate the F_{rad}, a one-dimensional radiative model, *Streamer* (Key 1999), was used. The *Streamer* is a radiative transfer model, containing the effects of cloud, realistic incoming solar radiation at the specific location and time, and albedos associated with various surface conditions. We supposed that the cloud appears when the relative humidity exceeds 85%. The difference of the calculated net radiation at p_{low} and p_{top} is regarded as F_{rad}.

We chose the same cases as in the previous subsection (Fig. 5). In each case, Δt is calculated by dividing the distance between the stations by the

Table 1. Average sea ice concentration in the area enclosed by thin lines in Fig. 3, top of the mixed layer (p_{top}), calculated net radiative flux (F_{rad}), and estimated turbulent heat flux of sensible and latent heat (F) in each case.

Case	1	2	3	4	5	6	7	8	9
Time at SH (UTC)	26Jan 18	29Jan 00	29Jan 06	01Feb 00	06Feb 21	10Feb 18	10Feb 21	11Feb 00	11Feb 03
Started at	YS	YS	YS	YS	YS	SO	SO	YS	SO
Sea-ice Cover (%)	45	48	46	49	62	65	65	65	71*
p_{top} (hPa)	780	870	870	840	850	965	920	945	955
F_{rad} (Wm^{-2})	-30	-20	-20	-20	-20	-20	-20	-10	0
F (Wm^{-2})	210	110	100	140	120	100	100	60	30

* Sea-ice concentration between SO and SH on Feb. 11 was nearly 100 % by the observation based on the sea-ice monitoring radar network on the Okhotsk coast operated by the Institute of Low Temperature Science, Hokkaido University.

average wind speed at YS (or SO) and SH in the mixed layer defined based on the profile at SH. Moreover, we take 1000 hPa as p_{low} in all cases, because the effect of local influence of the surface layer must be removed.

Table 1 shows the obtained turbulent heat fluxes. They gradually get smaller with time during our observational period, corresponding to the descending tendency of the mixed layer height of SH. This tendency may reflect the insulating effect of the heat transfer associated with the upward trend of the sea ice concentrations. The effect of the radiation process becomes gradually weaker, and its relative role on the mixed layer development becomes also small.

The estimated heat flux for each of *cases 2–4* is rather smaller than that of *case 1*. The increase of the ice concentration from *case 1* to *cases 2–4* is only 1–4%, whereas the reduction of the heat flux is nearly 100 W m^{-2}. In contrast, in spite of more than 15% increase of the sea-ice cover from *cases 2–4* to *cases 5–7*, few decrease of the heat flux is observed during this period. Also in *case 8*, reduction of the heat flux is confirmed although the increase of the ice concentration is not identified between *cases 5–7* and *8*. In each of *cases 2–4* and *8*, the YS's profile was considerably stable compared with *case 1* or *5* (Fig. 5). Because of the suppression of the convection due to the stable stability, the efficiency of the heat transfer between the ocean and atmosphere may be reduced. Further investigation is needed for the suppression of the mixed layer development associated with the stability of the air mass, and for characteristics of air-mass modification processes with shapes of vertical profiles.

In *case 9*, the significant reduction of the heat flux from about 100 W m^{-2} to 30 W m^{-2} was observed. In this case, the heat flux was estimated between SO and SH. As shown in Fig. 4b, the position of the *Soya* was near the coast of Hokkaido, and the sea-ice concentration between SO and SH was nearly 100%, which was confirmed by the observation using the sea-ice monitoring radar network on the Okhotsk coast operated by the Institute of Low Temperature Science, Hokkaido University. Therefore, the obtained value of the heat flux may reflect the heat released from the ice surface through inside the sea ice to the atmosphere.

It is difficult to decide the top of the mixed layer in *case 4*, as the profiles of the equivalent potential temperature in the free atmosphere over the mixed layer between YS and SH did not coincide (Fig. 5d). As mentioned previously, the YS's profile was considerably stable compared with other cases. In SH, a weak stable layer was identified between 910 hPa and 810 hPa above the mixed layer, and air temperature of the upper part of the weak stability layer of SH was colder than that of the corresponding height of YS. This temperature inversion between YS and SH may be caused by a mixing process between the mixed layer and free atmosphere above associated with an *entrainment* process, which is triggered by overshooting a buoyant thermal from the surface into the free atmosphere associated with free convection within the mixed layer (Stull 1988). The entrainment tends to occur when a stronger stable layer is heated from the lower boundary (Brümmer 1996). In this case, the top of the mixed layer is expected to exist between 910 hPa and 810 hPa, while we decided that the top of the mixed layer is 840 hPa. The heat flux is within in the range of 120–140 W m^{-2} if we choose any level between 910 hPa and 810 hPa as the top of the mixed layer. However, further study is needed for the estimation of the top of the mixed layer when the air-mass modification by the entrainment process occurs.

5. Conclusions and future works

Rawinsonde observation was performed in the southwestern part of the Sea of Okhotsk during winter in 1998 to investigate the atmospheric boundary-layer modification and to estimate the turbulent heat fluxes over the ice-covered ocean. Associated with cold air outbreaks, cold and stable air mass at the upstream station (YS or SO) was modified through heat flux release from warm

ocean surface. As a result, the mixed layer characterized by neutral stability was observed at the downstream station (SH), and the height gradually decreased through our observational period. Correspondingly, significant reduction of the turbulent fluxes of sensible and latent heat was also confirmed. Both decreases may reflect the increase of the insulative effect of the sea ice on heat transfer between the atmosphere and ocean. Estimated values of the total turbulent fluxes of the sensible and latent heat by the rawinsonde observation were ranged from 210 W m^{-2} for partly ice-covered ocean to 30 W m^{-2} for nearly perfect ice-covered condition, which are similar to those of other marginal ice zones (the Bering Sea, the Greenland Sea, and so on).

This observation had been continued to the following winters of 1999 and 2000, and performed for a longer period in both years than that of 1998. It is expected that we can promote a better understanding about the atmospheric modification processes and estimate more accurate values of the turbulent heat fluxes over the Sea of Okhotsk in the ice-covered condition through our analysis, which is in progress using these data.

Acknowledgments

We are grateful to the participants in this observation and to the crew of the ice breaker *Soya*. We would also thank Dr. N. Bond, Dr. T. Toyota, Prof. K. Yamazaki, and Mr. J. Inoue for useful discussion. Thanks are extended to Prof. S. Warren for his advice on the *Streamer*. The figures in this paper were produced by the Grid Analysis and Display System (GrADS) and GFD-DENNOU Library. This study was supported by the Grant-in-Aid for Scientific Research (No.09304044) from the Ministry of Education, Science, Sports and Culture of Japan and by Core Research for Evolutional Science and Technology (CREST) from Japan Science and Technology Corporation (JST).

References

Brümmer, B., 1996: Boundary-layer modification in wintertime cold-air outbreaks from the Arctic sea ice. *Bound.-Layer Meteor.*, **80**, 109–125.

Cavalieri, D.J. and C.L. Parkinson, 1987: On the relationship between atmospheric circulation and the fluctuations in the sea ice extents of the Bering and Okhotsk Seas. *J. Geophys. Res.*, **92**, 7141–7162.

Fang, Z. and J.M. Wallace, 1994: Arctic sea ice variability on a timescale of weeks and its relation to atmospheric forcing. *J. Climate*, **7**, 1897–1914.

Hein, P.F. and R.A. Brown, 1988: Observations of longitudinal roll vortices during Arctic cold air outbreaks over open water. *Bound.-Layer Meteor.*, **45**, 177–199.

Honda, M., Y. Tachibana and M. Wakatsuchi, 1994: The influences of the sea ice and the wind field on the winter air temperature variation in Hokkaido. *Proc. NIPR Symp. Polar Meteor. Glaciol.*, **8**, 81–94.

———, K. Yamazaki, Y. Tachibana and K. Takeuchi, 1996: Influence of Okhotsk sea-ice extent on atmospheric circulation. *Geophys. Res. Lett.*, **23**, 3595–3598.

———, K. Yamazaki, H. Nakamura and K. Takeuchi, 1999: Dynamic and thermodynamic characteristics of atmospheric response to anomalous sea-ice extent in the Sea of Okhotsk. *J. Climate*, **12**, 3347–3358.

Kellner, G., C. Wamser and R.A. Brown, 1987: An observation of the planetary boundary layer in the marginal ice zone. *J. Geophys. Res.*, **92**, 6955–6965.

Key, J.R., 1999: Streamer user's guide. *Technical report 96-01*, Department of Geography, Boston University.

Nagata, M. and M. Ikawa, 1988: Numerical experiments of the convergent cloud band over the Japan Sea. *Tenki*, **35**, 151–155, in Japanese.

National Snow and Ice Data Center, 1989: DMSP SSM/I brightness temperatures and sea ice concentration grids for the polar regions, 1987–. digital data available from nsidc@kryos.colorado.edu. *Technical report*, NSIDC Distributed Active Archive Center, University of Colorado at Boulder.

Okubo, H. and N. Mannoji, 1994: The influence of the sea ice distribution on the surface wind forecast by Japan Spectral Model. *Tenki*, **41**, 847–851, in Japanese.

Parkinson, C.L., 1990: The impact of the Siberian high and Aleutian low on the sea-ice cover of the Sea of Okhotsk. *Ann. Glaciol.*, **14**, 226–229.

Sasaki, H. and S. Deguti, 1988: Numerical experiments of the convergent band formed off the western coast of Hokkaido in winter. *Tenki*, **35**, 723–729, in Japanese.

Stull, R.B., 1988: *An Introduction to Boundary Layer Meteorology*. Kluwer Academic Publishers, 453pp.